

conclusion, however, that no conformational preference exists in solution. This is more in accord with the nmr results which indicate substantial but incomplete conformational averaging in $\text{Pt}(\text{en})_3^{4+}$.

Phosphate and similar anions cause substantial changes in the visible circular dichroism spectrum of $\text{Co}(\text{en})_3^{3+}$. It has been suggested that these are the consequence of changes in the conformations of the ligands,³⁰ an interpretation which is consistent with the effects of phosphate on the nmr spectra.^{13,24}

Calculations. Attempts have been made to obtain more reliable estimates of the relative energies of the various conformational configurations by more sophisticated calculations of the type initiated by Corey and Bailar. Although the results are highly dependent on the force field adopted, a number of interesting conclusions emerge.^{14,31} The enthalpy differences among the configurations decrease as the size of the metal ion increases since the interligand interactions are reduced, although there is some increase in strain energy in each ligand. Since the statistical entropy contribution to the free energy remains constant, the net result is that the $\Lambda(\delta\delta\lambda)$ configuration is decidedly of lowest free energy in the larger complexes of nickel(II)

(30) A. J. McCaffery, S. F. Mason, and B. J. Norman, *Chem. Commun.*, 49 (1965); R. Larsson, S. F. Mason, and B. J. Norman, *J. Chem. Soc. A*, 301 (1966); S. F. Mason and B. J. Norman, *ibid.*, A, 307 (1966).

(31) J. R. Gollgoly and C. J. Hawkins, *Inorg. Chem.*, 9, 576 (1970); M. Snow, personal communication.

and ruthenium(II) but probably of nearly the same free energy as the $\Lambda(\delta\delta\delta)$ configuration in the smallest complex of cobalt(III). In every case the energy barrier to ring inversion is only 5-7 kcal mole⁻¹, which accounts for the absence of dynamic effects in the nmr spectra.

Conclusions

The model advanced by Corey and Bailar for the conformational analysis of tris(ethylenediamine)-metal complexes is generally verified by the nmr spectra of the complexes. The ligands are in rapid conformational equilibrium, with the δ conformer more stable than the λ conformer in the Λ configuration by 0.3-0.6 kcal, depending on the size of the metal ion. A statistical entropy effect results in the $\Lambda(\delta\delta\lambda)$ configuration being most abundant in solution, at least for the larger complexes. The very different nmr spectra of the various complexes result from large variations in chemical shielding and do not reflect substantially different stereochemical properties.

I wish to acknowledge the substantial contributions made to this work by my students and colleagues, particularly Sr. Helen Elsbernd and Lucille H. Novak for much of the experimental work, Professor Theodore L. Brown for many instructive discussions, and Dr. C. J. Hawkins and Professor Charles Reilley for enlightening correspondence. Grateful acknowledgment for financial support is made to the National Institutes of Health under Grant GM 16168 and to the donors of the Petroleum Research Fund, administered by the American Chemical Society.

Atomic Fluorescence Flame Spectrometry[†]

JAMES D. WINEFORDNER

Department of Chemistry, University of Florida, Gainesville, Florida 32601

Received August 6, 1970

In atomic fluorescence flame spectrometry, the liquid sample to be analyzed is introduced through a "nebulizer" into a flame as a mist. The heat of the flame evaporates the solvent and vaporizes the analyte. The combustion flame acts as a convenient and relatively efficient atom-producing plasma. The atoms are then optically excited by some source and their fluorescence is observed.

The first reference to fluorescence of atomic vapors in flames was in 1924, when Nichols and Howes¹ observed the fluorescence of Ca, Sr, Ba, Li, and Na in a Bunsen burner flame. In 1927, Badger² published a classic paper on the atomic fluorescence of Tl, Hg, Mg, Cu, Ag, Cd, and Na in flames; in 1962, Alkemade³

mentioned the possible analytical use of atomic flame fluorescence spectrometry; and in 1964, Winefordner and Vickers⁴ published the first paper on this phenomenon as an analytical method.

In Figure 1, several fluorescence processes of possible analytical use are indicated. The fluorescence of greatest analytical interest is the first resonance transition ($1 \rightarrow 0$). In *resonance fluorescence*, the absorbed and emitted photons are of the same frequency.

Stepwise line fluorescence (Figure 1, process b) results when excitation is to a higher energy state which is deactivated to a lower excited state before emission. To date, this has been of little analytical use since the radiant flux of most commonly used sources at wavelengths corresponding to second and higher absorptions is low and the efficiency of populating the first excited state from higher states is small. *Direct line fluorescence*

(4) J. D. Winefordner and T. J. Vickers, *Anal. Chem.*, 36, 161 (1964).

[†] Research sponsored by AFOSR (AFSC), USAF Grant 70-1880B.

(1) E. L. Nichols and H. L. Howes, *Phys. Rev.*, 23, 472 (1924).

(2) R. M. Badger, *Z. Phys.*, 55, 56 (1929).

(3) C. T. J. Alkemade in "Proceedings of the Xth Colloquium Spectroscopicum Internationale," E. R. Lippincott and M. Margoshes, Ed., Spartan Books, Washington, D. C., 1963.

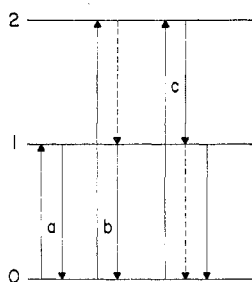


Figure 1. Types of atomic fluorescence: (a) resonance fluorescence; (b) stepwise-line fluorescence; (c) direct-line fluorescence.

(Figure 1, process c) results when an atom is excited to a state which fluoresces to a state above the ground state. In both stepwise and direct line fluorescence, the emission is at a different wavelength than the absorption.

Finally, *sensitized fluorescence* occurs when an excited species (donor) transfers energy to another species (acceptor), which then fluoresces. This process has no analytical use in flames because of the difficulty of producing a sufficiently high concentration of donors in the flame.

Qualitatively, one would expect that the radiance of the fluorescence would be related to the radiance of the exciting radiation, the fraction of this radiation absorbed, the fluorescence efficiency, and the fraction of the fluorescence which is reabsorbed. It is the purpose of this Account to explore these relationships and to discuss the practicality and limitations of atomic fluorescence flame spectrometry as an analytical tool.

Theoretical Considerations

Radiance of Atomic Fluorescence.⁵⁻⁸ The radiance of atomic fluorescence, B_F , is the radiant flux (ergs per second) of fluorescence (due to the analyte atoms) per square centimeter of flame gases (the fluorescence area) per steradian (the solid angle of flame gases toward the measurement system). The measured photodetector signal of an atomic fluorescence flame spectrometer depends directly upon B_F over a wide range of B_F values.⁹ Useful expressions relating the radiance B_F to spectral parameters and to atomic analyte concentration in the flame gases have been derived with the following assumptions: (i) the flame is rectangular, $L \times l$ cm² (see Figure 2), and is irradiated by a parallel homogeneous light beam with a rectangular cross section, $L \times H$ (H is the height of the illuminating beam); (ii) the flame containing the analyte atomic vapor is surrounded by a metal-free mantle flame with the same flame gas temperature and composition to assure a uniform temperature distribution inside the

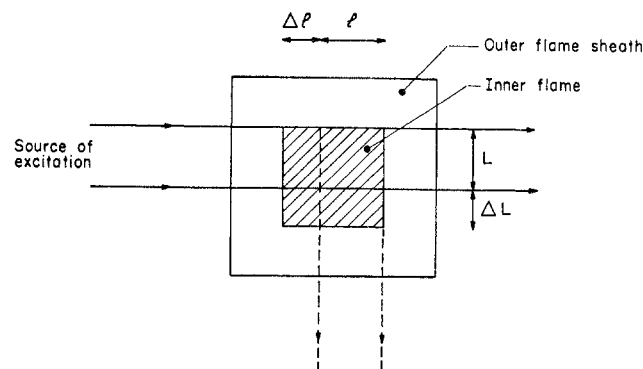


Figure 2. Cross-sectional area of the flame, of the irradiating light beam, and of the fluorescence light beam as seen from above. The inner (with metal atoms) and outer flames (without metal atoms) are shown.

inner flame; (iii) because of assumption ii, the atomic concentration of metal atoms in the ground state, n_0 , is constant at all points in the measured volume; (iv) the fluorescence radiation is observed in a *small* solid angle in the direction perpendicular to the irradiating light beam and the flame axis; (v) fluorescence is excited with either a continuum light source (the half-width of the spectral distribution of the source is much greater than the absorption line half-width), or with a narrow line light source (the half-width of the spectral line of the exciting source is narrower than the half-width of the absorption line); and (vi) the atomic vapor is either dilute or concentrated, and so only *limiting expressions* will be given. The expressions to be given are useful for *evaluating spectral parameters*, e.g., quantum yields, damping constants, free-atom fractions, etc., and for *predicting the shapes of analytical curves* ($\log B_F$ vs. \log sample concentration) and *limits of detection* in analytical atomic fluorescence flame spectrometry. Resonance fluorescence radiance expressions have already been derived by Hooymayers,⁷ Zeegers, Smith, and Winefordner,⁵ and Zeegers and Winefordner,⁸ and the expressions given here are taken from these papers.

For a continuum source of excitation (C) and for dilute (L) analyte atomic vapor, B_{FCL} (radiance of resonance fluorescence with continuum source and low analyte concentration) is given by eq 1, and for a con-

$$B_{FCL} = C_1 \kappa_0 n_0 f_{01} L \Delta \lambda_D B_{C\lambda_0} Y (\Omega/4\pi) \quad (1)$$

tinuum source and for concentrated (H) analyte atomic vapor, B_{FCH} (radiance of resonance fluorescence with continuum source and high analyte concentration) is given by eq 2.

$$B_{FCH} = 2B_{C\lambda_0} \Delta \lambda_D a Y \left(\frac{\Omega}{4\pi} \right) \left[\frac{C_2 L}{\pi^{1/2} l} \right]^{1/2} \times \left[\frac{(L + \Delta L)^{1/2} - (\Delta L)^{1/2}}{L^{1/2}} \right] \left[\frac{(l + \Delta l)^{1/2} - (\Delta l)^{1/2}}{l^{1/2}} \right] \quad (2)$$

For a narrow line source (L) and for dilute (L) analyte atomic vapor, the radiance of atomic fluorescence B_{FLL} is given by eq 3, and for a narrow line

(5) P. J. T. Zeegers, R. Smith, and J. D. Winefordner, *Anal. Chem.*, **40** (13), 26A (1968).

(6) C. T. J. Alkemade in "Proceedings of Atomic Absorption Conference, Sheffield, England," July 1969, Butterworths, London, 1971.

(7) H. P. Hooymayers, *Spectrochim. Acta, Part B*, **23**, 567 (1968).

(8) P. J. T. Zeegers and J. D. Winefordner, *ibid.*, in press.

(9) J. D. Winefordner, V. Svoboda, and L. Cline, *Crit. Rev. Anal. Chem.*, **1**, 232 (1970).

$$B_{FLL} = \kappa_0 n_0 f_{0u} L \delta_0 B_L Y (\Omega/4\pi) \quad (3)$$

source (L) and for a concentrated (H) analyte atomic vapor, the radiance of atomic fluorescence B_{FLH} is given by eq 4.

$$B_{FLH} = 2B_L Y \left(\frac{\Omega}{4\pi} \right) \left[\frac{a}{\pi^{1/2} \kappa_0 n_0 f_{0u} L} \right]^{1/2} \times \left[\exp(-\kappa_0 n_0 f_{0u} \delta_0 \Delta l) \right] \left[\frac{(L + \Delta L)^{1/2} - (\Delta L)^{1/2}}{L^{1/2}} \right] \quad (4)$$

The symbols in the above equations are

C_1	$\pi^{1/2}/2 (\ln 2)^{1/2}$, no units
C_2	$\pi^{1/2}/\ln 2$, no units
κ_0	$C_2 X \lambda_0^2 / \pi c \Delta \lambda_D$, cm^2
X	$\pi e^2 / mc$, $\text{cm}^2 \text{sec}^{-1}$
e, m	charge and mass of electron, esu and g
c	speed of light, cm sec^{-1}
λ_0	peak absorption line wavelength, cm
$\Delta \lambda_D$	Doppler half-width of absorption line, nm
a	damping constant, $(\ln 2)^{1/2} \Delta \lambda_C / \Delta \lambda_D$, no units
$\Delta \lambda_C$	collisional half-width of absorption line, nm
Ω	solid angle of excitation radiation collected by entrance optics and impinging on flame, sr
Y	fluorescence quantum yield, no units
L	fluorescence path length, cm
l	absorption path length, cm
f_{0u}	absorption oscillator strength for ground state to upper state transition, no units
Δl	region of inner flame over which fluorescence is <i>not</i> measured (see Figure 2), cm
ΔL	region of inner flame which is <i>not</i> excited (see Figure 2), cm
δ_0	factor to account for finite width of narrow line source and for absorption line profiles, no units
$B_{C\lambda_0}$	spectral radiance of continuum source at λ_0 , $\text{erg sec}^{-1} \text{cm}^{-2} \text{sr}^{-1} \text{nm}^{-1}$
B_L	radiance of narrow line source at λ_0 , $\text{erg sec}^{-1} \text{cm}^{-2} \text{sr}^{-1}$

If the flame cell is completely illuminated, *i.e.*, $\Delta L = 0$ in Figure 2, and if atomic fluorescence over the entire flame cell is observed, *i.e.*, $\Delta l = 0$ in Figure 2 (no inner filter effect), then the last two terms (in brackets) in eq 4 and in eq 2 reduce to unity.

Growth Curves in Atomic Fluorescence Flame Spectrometry. Growth curves ($\log B_F$ vs. $\log n_0$) for atomic fluorescence flame spectrometry with a continuum and with a line source of excitation and for various cell configurations can only be obtained by use of general expressions for the atomic fluorescence radiance B_F .^{5,7-9} The limiting expressions given above are only useful for defining the limiting (asymptotic) slopes of the growth curves. Some hypothetical growth curves (assuming measurement of a resonance line) which obey the above expressions for the limiting cases are given in Figure 3. It should be stressed that all growth curves in atomic fluorescence flame spectrometry, whatever the source of excitation and whatever the sample cell geometry, have a slope of unity for dilute atomic vapors, *i.e.*, the atomic fluorescence radiance, B_F , is proportional to ground-state atomic concentration, n_0 . Atomic fluorescence flame spectrometry is therefore of *greatest analytical* use in trace analysis, *i.e.*, dilute solutions of the analyte sprayed into the flame.

Analytical Curves in Atomic Fluorescence Flame Spectrometry.⁵ Analytical curves (\log instrumental signal, S , vs. \log analyte concentration, C , sprayed into the flame) have the same shape as growth curves except as modified by nonlinearity between analyte concen-

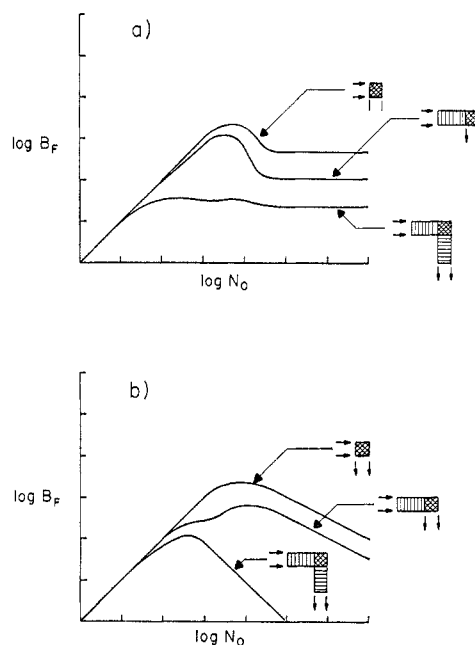


Figure 3. Hypothetical growth curves in atomic fluorescence flame spectrometry for a hypothetical resonance line: (a) continuum light source; (b) line light source. The cross-hatched region is the region excited and measured. In the vertical region inner filter effects cause a reduced source radiance, and in the horizontal region self-absorption causes a reduced fluorescence signal.

tration in the flame gases, n_0 , and analyte concentration introduced into the flame gases, C . The relationship between n_0 and C is given by eq 5, where $N_A = \text{Avogadro's number, atoms mole}^{-1}$;

$$n_0 = (N_A F \epsilon \beta / e_t Q) C \quad (5)$$

F = solution flow rate through nebulizer, $\text{cm}^3 \text{sec}^{-1}$; ϵ = efficiency of converting sample solution into atoms, molecules, and ions, no units; β = efficiency of converting analyte species into atoms, no units; e_t = flame gas expansion factor, no units; Q = flow rate of unburnt gases into flame, $\text{cm}^3 \text{sec}^{-1}$; and C = analyte concentration in sample solution, mole cm^{-3} . If in eq 5 all terms in the parentheses are independent of C , then the analytical curve should have *exactly the same shape as the corresponding growth curve*. However, the solution flow rate, F , will generally decrease at large values of C due to an increase in viscosity of the solution. Also, the efficiency of aspiration, ϵ , will generally decrease at high values of C due to a reduced efficiency of vaporizing solute particles in the flame gases. If the sample solution is nebulized into a spray chamber, the efficiency of the spray chamber (*i.e.*, the ratio of the amount of spray leaving the chamber and ending up in the flame to the amount of spray entering the spray chamber) may also change at high values of C . Finally, the free-atom fraction β will often decrease at low analyte concentrations due to an increase in ionization of a dilute atomic gas as C decreases. However, although β may be much less than unity due to compound formation between the analyte atoms and flame gas radicals, β is still *independent* of C . (β for compound formation of the metal with flame gas

products depends *only* upon the *metal*, the flame gas *composition*, and the flame gas *temperature*.)

Therefore, due to the above changes in solution flow rate, F , efficiency of aspiration, ϵ , and free-atom fraction, β , analytical curves may have slightly greater slopes at low analyte concentrations and slightly lesser slopes at high analyte concentration than the growth curves.

Instrumental System

The instrumental system for atomic fluorescence flame spectrometry is similar to the systems used in both ordinary fluorimetry of organic molecules and in flame photometry. A block diagram of an atomic fluorescence flame spectrometer is given in Figure 4. The instrument consists simply of an excitation source, a flame atomizer, an appropriate entrance optics system, a monochromator, a photodetector, and an electronic system.

The excitation source can be either narrow line lamps (*e.g.*, radiofrequency or microwave-powered electrodeless discharge tubes, high-intensity hollow cathode lamps, and metal vapor discharge arc lamps) or continuum lamps (*e.g.*, xenon arc lamps). The most popular source in atomic fluorescence flame spectrometry has been electrodeless discharge tubes which can be fabricated for virtually all elements in the periodic table.

The nebulizer-burner system can be either the conventional total consumption nebulizer-burner commonly used for flame emission spectrometry or the conventional chamber-type nebulizer-laminar flow burner commonly used for atomic absorption flame spectrometry. The former burner produces rather turbulent diffusion flames with high-burning-velocity gas mixtures, such as $\text{H}_2\text{-O}_2$ and $\text{C}_2\text{H}_2\text{-O}_2$. The latter burner produces more laminar, premixed flames with low burning velocity mixtures, such as $\text{C}_2\text{H}_2\text{-air}$, $\text{C}_2\text{H}_2\text{-N}_2\text{O}$, $\text{H}_2\text{-air}$, propane-air, and $\text{H}_2\text{-O}_2\text{-Ar}$. The most popular flames for atomic fluorescence spectrometry have been turbulent $\text{H}_2\text{-air}$, turbulent $\text{H}_2\text{-Ar}$ -entrained air, premixed $\text{H}_2\text{-N}_2\text{O}$, premixed $\text{H}_2\text{-air}$, premixed $\text{C}_2\text{H}_2\text{-N}_2\text{O}$, and premixed $\text{H}_2\text{-O}_2\text{-Ar}$. The premixed $\text{C}_2\text{H}_2\text{-N}_2\text{O}$ flame has a high temperature, a low burning velocity, and a large reducing interconal zone, and so this flame results in the least amount of solute vaporization interferences (*i.e.*, decrease in the efficiency of aspiration, ϵ , due to interferences in the sample). On the other hand, the premixed $\text{H}_2\text{-O}_2\text{-Ar}$ flame results in the lowest flame background and the greatest quantum yields of the group of flames.

Recently nonflame atomizers (*e.g.*, graphite furnaces in an inert atmospheres and heated metal loops with sample solution in inert gas atmospheres) have been used rather than flames as atomizers in atomic fluorescence spectrometry. Such systems result in efficient atomization for many elements and in larger quantum yields than flames, but are not as simple to use as flames.

The entrance optics system is needed for focusing the exciting radiation upon the flame gases and focusing

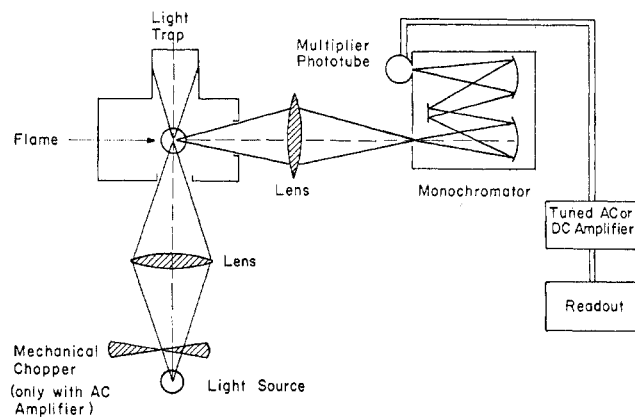


Figure 4. Schematic diagram of an atomic fluorescence flame spectrometer.

the fluorescence from the flame gases onto the entrance slit of a small monochromator with large aperture (generally Czerny-Turner grating monochromators are used). The electronic measurement system can be as simple as a dc electrometer-recorder readout or as elaborate as a phase-sensitive amplifier-recorder readout system. In the latter case, it is also necessary to modulate the radiation from the exciting source. This is often done by means of a mechanical chopper.

Analytical Studies

Limits of Detection. Atomic fluorescence from 30 elements has been observed by more than one investigator. Because only flame noise and phototube shot noise are usually significant, very low limits of detection (analyte concentration resulting in a signal-to-noise ratio of 2) have resulted for several elements. In Table I, the state-of-the-art limits of detection for 30 elements determined by atomic fluorescence flame spectrometry with either a continuum (AFC) or a line source (AFL) are given. Because the limits of detection for several elements compare favorably with or are better than those obtained with more conventional methods such as atomic absorption and atomic emission flame spectrometry and inorganic absorption spectrophotometry and spectrofluorimetry and with exotic methods like neutron activation and spark source mass spectroscopy, numerous applications of this new sensitive method should be forthcoming. As more intense, stable sources and better atomizers become available, even lower limits of detection should result.

Interferences. Because atomic fluorescence flame spectrometry involves the measurement of narrow fluorescence lines (order of 0.1 \AA half-width), spectral (line overlap) interferences are small. The *major interferences in any flame method are concerned with the production of the atomic vapor*. Any concomitant resulting in a change in either sample solution flow rate, F , or in the efficiency of aspiration, ϵ , or in the free-atom fraction, β , will produce a change in fluorescence signal and result in an interference. Such interferences can be minimized by utilizing efficient nebulizers and hot, low-burning-velocity flames.

Agreement between Theory and Experiment. Ex-

Table I
Limits of Detection for Several Elements in Atomic Fluorescence Flame Spectrometry with a Continuum (AFC) and a Line (AFL) Light Source

Element	Wavelength, ^w Å	Flame ^z	Limit of detection, µg ml ⁻¹			
			AFC	Ref	AFL	Ref
Ag	3281	H/A	0.001	a, b	0.0001	c
Al	3092-3962	H/A-H/N	4	d	2	e
As	1972-1937	H/A	2	d	0.1	e
Au	2676	H/O-H/A	4	f	0.05	g
Be	2349	A/N			0.01	h, i
Bi	3068	H/A	0.5	d	0.005	j
Ca	4227	H/A	0.02	d	0.02	c
Cd	2288	H/A-H/O	0.01	d	0.000001	c
Co	2407	H/A	0.02	d	0.005	k
Cr	3579	H/A	10	g	0.05	e
Cu	3247	H/A	0.01	d	0.001	l, m
Fe	2483	H/A	0.04	d	0.008	e
Ga	4172	H/A	0.1	d	0.007	d
Ge	2651	H/A	2	d	2	d
Hg	2537	H/A			0.08	n
In	4105-4511	H/A	2	g	0.1	c
Mg	2852	H/A-A/A	0.004	o	0.001	p
Mn	2795	H/A	0.003	d	0.006	c
Na	5896	H/A	0.008	d		
Ni	2320	H/O/Ar-H/A	0.5	q	0.003	r
Pb	2833-4058	H/A	0.6	d	0.02	m
Rh	3692	H/A	10	g	3	g
Sb	2311	H/A-P/A	300	g	0.05	s
Se	1960	H/A-A/A	4	d	1	o
Si	2040	P/A			0.1	t
Sn	3034	H/A			0.05	u
Sr	4607	H/A			0.03	c
Te	2143	H/A-A/A	8	d	0.05	t
Tl	3776	H/A	0.07	a, b, v	0.006	d
Zn	2138	H/A	0.02	d	0.00005	c

^a D. R. Demers and D. W. Ellis, *Anal. Chem.*, **40**, 860 (1968). ^b D. W. Ellis and D. R. Demers, *Advan. Chem. Ser.*, **No. 73** (1968). ^c K. E. Zacha, M. P. Bratzel, J. D. Winefordner, and J. M. Mansfield, *Anal. Chem.*, **40**, 1233 (1968). ^d A. Hell and B. Ricchio, talk given at Pittsburgh Conference on Analytical Chemistry and Applied Spectroscopy, Cleveland, Ohio, 1970. ^e R. M. Dagnall, M. R. G. Taylor, and T. S. West, *Spectrosc. Lett.*, **1**, 397 (1968). ^f C. Veillon, J. M. Mansfield, M. P. Parsons, and J. D. Winefordner, *Anal. Chem.*, **38**, 204 (1966). ^g D. C. Manning and P. Heneage, *At. Absorption Newslett.*, **7**, 80 (1968). ^h M. P. Bratzel, R. M. Dagnall, and J. D. Winefordner, *Anal. Chem.*, **41**, 1527 (1969). ⁱ D. N. Hingle, G. F. Kirkbright, and T. S. West, *Analyst*, **93**, 522 (1968). ^j R. M. Dagnall, K. C. Thompson, and T. S. West, *Talanta*, **14**, 1467 (1967). ^k B. Fleet, K. V. Liberty, and T. S. West, *Anal. Chim. Acta*, **45**, 205 (1969). ^l J. I. Dinnin, *Anal. Chem.*, **39**, 1491 (1967). ^m D. C. Manning and P. Heneage, *At. Absorption Newslett.*, **6**, 124 (1967). ⁿ R. F. Browner, R. M. Dagnall, and T. S. West, *Talanta*, **16**, 75 (1969). ^o M. S. Cresser and T. S. West, *Spectrosc. Lett.*, **2**, 9 (1969). ^p T. S. West and X. K. Williams, *Anal. Chim. Acta*, **42**, 29 (1968). ^q R. Smith, C. M. Stafford, and J. D. Winefordner, *Can. Spectrosc.*, **14**, 2 (1969). ^r J. Matousek and V. Sychra, *Anal. Chem.*, **41**, 518 (1969). ^s R. M. Dagnall, K. C. Thompson, and T. S. West, *Talanta*, **14**, 1151 (1967). ^t R. M. Dagnall, K. C. Thompson, and T. S. West, *ibid.*, **14**, 557 (1967). ^u R. F. Browner, R. M. Dagnall, and T. S. West, *Anal. Chim. Acta*, **46**, 207 (1969). ^v D. W. Ellis and D. R. Demers, *Anal. Chem.*, **38**, 1943 (1965). ^w If more than one wavelength is given, the first wavelength is for AFC and the second is for AFL. If only one wavelength is given, it corresponds to both AFC and AFL, assuming limits of detection for both methods are given. ^x H/A = hydrogen-air flame; H/N = hydrogen-nitrous oxide flame; H/O/Ar = hydrogen-oxygen-argon flame; A/A = acetylene-air flame; A/N = acetylene-N₂O flame; P/A = propane-air flame. If more than one flame type is given, the first flame type is for AFC and the second for AFL. If only one flame type is given, it is for both AFC and AFL, assuming limits of detection are given for both methods.

perimental analytical curves agree qualitatively with the shapes predicted by eq 1-4. Zeegers and Winefordner⁸ have carefully measured analytical curves for Mg (2852 Å) in a square premixed C₂H₂-air flame with a flame sheath and have found excellent agreement with the results predicted by theory (eq 1-4); the agreement was excellent even for cases of incomplete excitation ($\Delta L \neq 0$ in Figure 2) and incomplete measurement of fluorescence ($\Delta l \neq 0$ in Figure 2).

Fundamental Studies

Quantum Yield.¹⁰⁻¹⁷ If the fraction of absorbed radiant flux which is reemitted as atomic fluorescence at frequency ν_{ul} is measured, the atomic fluorescence

power yield Y' is given by eq 6, where Φ_F = radiant

$$Y' = \frac{\Phi_F}{\Phi_A} = Y \left(\frac{\nu_{ul}}{\nu_{ou}} \right) = \left(\frac{\nu_{ul}}{\nu_{ou}} \right) \left(\frac{\alpha A_{ul}}{\sum_i A_{ui} + \sum_j k_{xj} [X_j]} \right) \quad (6)$$

(10) D. R. Jenkins, *Proc. Roy. Soc., Ser. A*, **293**, 493 (1966).

(11) D. R. Jenkins, *ibid.*, *Ser. A*, **303**, 453 (1968).

(12) D. R. Jenkins, *ibid.*, *Ser. A*, **303**, 467 (1968).

(13) D. R. Jenkins, *ibid.*, *Ser. A*, **306**, 413 (1968).

(14) H. P. Hooymayers and C. T. J. Alkemade, *J. Quant. Spectrosc. Radiat. Transfer*, **6**, 501 (1964).

(15) H. P. Hooymayers and P. L. Lijnse, *ibid.*, **9**, 995 (1969).

(16) D. R. Jenkins, *Spectrochim. Acta, Part B*, **25**, 47 (1970).

(17) S. J. Pearce, L. de Galan, and J. D. Winefordner, *ibid.*, *Part B*, **23**, 793 (1968).

Table II
Calculated Fluorescence Quantum Yields for Several Atoms in Several Flames¹⁶

Flame composition ^a	Temp, °K	Fluorescence quantum yield				
		Li	Na	K	Tl	Pb
H/O/Ar, 2:1:10	1800	0.15	0.75	0.37	0.33	0.22
H/O/N, 6:1:4	1800	0.015	0.049	0.049	0.099	0.10
H/O/N, 2:1:4	2100	0.021	0.066	0.047	0.070	0.079
H/O/N, 1:1:4	1600		0.044	0.03	0.051	0.069
A/O/N, 0.4:1:4	2200	0.017	0.042	0.028	0.042	0.067

^a Flow rate ratios of gases.

flux fluoresced by analyte atom, erg sec⁻¹; Φ_A = radiant flux absorbed by analyte atom, erg sec⁻¹; Y = quantum yield, *i.e.*, number of photons of ν_{ul} emitted as fluorescence to number of photons of ν_{0u} absorbed, no units; A_{ul} = Einstein coefficient of spontaneous emission for transition $u \rightarrow l$, sec⁻¹; A_{ui} = Einstein coefficient of spontaneous emission for transition $u \rightarrow i$, sec⁻¹; k_{x_j} = second-order quenching rate constant for quenching of excited analyte due to collision with quenching X_j , cm³ sec⁻¹; $[X_j]$ = concentration of quencher X_j , cm⁻³; ν_{ul} = frequency of fluorescence peak for transition $u \rightarrow l$, sec⁻¹; ν_{0u} = frequency of absorption peak for transition $0 \rightarrow u$, sec⁻¹; α = factor to account for reabsorption of fluorescence by analyte atoms, no units.

The second-order rate constant for quenching, k_{x_j} , is given by eq 7, where σ^2 = quenching cross-section

$$k_{x_j} = \sigma^2 \left[8\pi kT \left(\frac{1}{m_A} + \frac{1}{m_{x_j}} \right) \right]^{1/2} \quad (7)$$

between analyte atom and quencher X_j , cm²; k = Boltzmann constant, erg °K⁻¹; T = flame temperature, °K; m_A = mass of analyte atom, g; m_{x_j} = mass of quencher, g. For resonance absorption-fluorescence, $\nu_{ul} = \nu_{0u}$. Also for dilute atomic vapors, the fraction of reabsorption $\alpha \simeq 1$.

Measurement of power yields as a function of the flame gas composition, $[X_j]$, and knowledge of the transition probability, A_{ul} , allows estimation of the second-order quenching rate constants, k_{x_j} , for a given analyte atom and a given quencher, *e.g.*, CO₂, CO, N₂, H₂O, O₂, etc. From the values of the second-order quenching rate constants, k_{x_j} , quenching cross sections, σ^2 , for the quenching process can then be evaluated (from eq 7).

Using quenching cross sections previously evaluated,¹⁰⁻¹⁵ Jenkins¹⁶ calculated the quantum yields, Y , for Na, Li, K, Tl, and Pb in a variety of analytical flames; the yields are given in Table II. The data in Table II clearly show that the *types of flame giving the largest quantum yields are those diluted with inert gases* because quenching processes are negligibly small for inert gases compared with N₂, CO, and CO₂. Because the quenching rates for H₂ and for O₂ are appreciable, the quantum yield for a given atom is greatest in stoichiometric flames containing an inert gas.¹⁸

Jenkins¹⁶ noted that as little as 5% N₂ in a stoichio-

metric inert gas flame (temperature of 1600°K) reduced the quantum yield of Na 5890/5896 Å doublet to *one-sixth* of its value. Pearce, de Galan, and Winefordner¹⁷ also indicated that the use of turbulent, unpremixed, unshielded diffusion flames resulted in uniformly low values in the quantum yields due to a great amount of air entrainment from the atmosphere. Therefore, if H₂-O₂-Ar flames are to be used for analytical studies, they should be surrounded by a flame sheath of the same composition as the inner flame and also by an outer argon sheath (surrounding the flame sheath) if possible.

***a* Parameter.**^{7,8} The *a* parameter (also called damping constant) is defined by $a = (\ln 2)^{1/2} \Delta\lambda_C / \Delta\lambda_D$ for the analyte atom in the flame gas of concern. The concentration at the intersection of the high and low concentration asymptotes of growth curves and also of analytical curves is dependent upon the value of the *a* parameter. Also the shape of the intersection region is dependent upon the magnitude of the *a* parameter, but this fine feature is only apparent when using the general expressions for B_F rather than the limiting equations given above.

The *a* parameter can be estimated graphically from the intersection point of the high and low concentration asymptotes of the analytical (growth) curve obtained in atomic fluorescence flame spectrometry with a continuum source. Combining eq 1 and 2 gives eq 8,

$$(\kappa_0 n_0 f_{0u})_I = \left[\frac{4a}{(\pi)^{1/2} lL} \right] \times [(L + \Delta L)^{1/2} - (\Delta L)^{1/2}] [(l + \Delta l)^{1/2} - (\Delta l)^{1/2}] \quad (8)$$

where subscript I refers to the intersection point. If $\kappa_0 n_0 f_{0u}$ is known from an integrated atomic absorption measurement and if the flame dimensions are known, then it is possible to determine the *a* parameter for a given atom in a given flame. The magnitude of the *a* parameter is quite insensitive to atomic concentration and even to flame gas temperature but does depend upon the atom type and the flame gas composition. If the *a* parameter and the flame temperature are known (temperature to estimate the Doppler half-width), then the collisional half-width, $\Delta\lambda_C$, can be estimated as well as the effective collisional cross section. It should again be stressed that the *shapes of growth curves in atomic fluorescence* (also in atomic absorption and in atomic emission flame spectrometry) depend upon the value of the *a* parameter (*a* parameters vary from about 0.5 to 2 for most atoms in most flames).

(18) Jenkins¹⁶ states that Tl is the only known case where H₂ had no appreciable effect on the quantum yield.